doi: 10.4149/gpb_2020033

miRNAs regulating the expressions of NTF3, GNG2 and ITGA7 are involved in the pathogenesis of abdominal aortic aneurysm in mice

Shujie Gan[1], Weijun Shi[2] and Jingdong Tang[2]

[1] *Department of Vascular Surgery, Shanghai General Hospital, Shanghai Jiao Tong University School of Medicine, Shanghai, China*
[2] *Department of Vascular Surgery, Shanghai Pudong Hospital, Fudan University Pudong Medical Center, Shanghai, China*

Abstract. Abdominal aortic aneurysm (AAA) is a life-threatening vascular disease, but effective treatment strategies remain lacking. The objective of this study was to screen underlying therapeutic targets by investigating the molecular mechanisms of AAA using mouse models. The mRNA (GSE109639) and miRNA (GSE51229 and GSE54943) expression profiles of mouse AAA models were downloaded from Gene Expression Omnibus database. A total of 1367 differentially expressed genes (DEGs) were identified between AAA and sham group, 490 of which were used for constructing the Protein-Protein Interaction (PPI) network. *NTF3*, *GNG2* and *ITGA7* in the PPI network were suggested to be hub genes according to their ranking of topological features. Furthermore, hub gene *GNG2* was enriched in module 1, while *ITGA7* was enriched in module 3. Eighteen differentially expressed miRNAs (DEMs) were shared in two datasets, 6 of which were predicted to regulate 130 DEGs (i.e. mmu-miR-677-*ITGA7*, mmu-miR-350-*NTF3* and mmu-miR-292-3p-*GNG2*) to establish the miRNA-mRNA regulatory network. Function enrichment analysis showed *NTF3* was involved in cell motion and MAPK signaling pathway; *ITGA7* affected extracellular matrix (ECM)-receptor interaction; *GNG2* participated in cell proliferation and chemokine signaling pathway. In conclusion, miRNAs regulating the expressions of *NTF3*, *GNG2* and *ITGA7* may represent underlying targets for treatment of AAA.

Key words: Abdominal aortic aneurysm — microRNAs — Inflammation — Cell proliferation

Introduction

Abdominal aortic aneurysm (AAA), characterized by focal dilatation of the diameter of the abdominal aorta by at least 50% or to more than 3 cm (Kent 2014), is a common vascular disease for population aged over 65 years (Dereziński et al. 2017). AAA is usually asymptomatic, but once ruptures, approximately 90% of patients succumb to sudden death (Johansson and Swedenborg 2010; Kent 2014), which make AAA as a serious threat to human public health. However, there are currently no effective therapies (except surgery that was only recommended for patients with diameters above 5–5.5 cm) to block AAA development and prevent rupture (Lieberg et al. 2017). Therefore, there is urgent need to deeply explore the mechanisms of AAA to find underlying targets for developing novel, effective therapeutic strategies.

MicroRNAs (miRNAs), noncoding RNAs with about 22 nucleotides in length, have been demonstrated to play important roles in various diseases by regulating the expression of target genes through inhibition of their translation or transcript degradation and thus they may represent potential targets for treatment of AAA. This hypothesis has been verified in AAA animal model experiments by some scholars. For example, using two murine models [the porcine pancreatic elastase (PPE) infusion model in C57BL/6 mice and the angiotensin II (Ang II) infusion model in ApoE-/-mice)], Maegdefessel et al. (2012) found that miR-29b was significantly downregulated in AAA. Further mechanism study indicated that miR-29b may be a protective response, overexpression of

Electronic supplementary material. The online version of this article (doi: 10.4149/gpb_2020033) contains Supplementary Material.

Correspondence to: Jingdong Tang, Department of Vascular Surgery, Shanghai Pudong Hospital, Fudan University Pudong Medical Center, No. 2800 Gongwei Road, Shanghai 201399, China
E-mail: jingdongtang20195@aliyun.com

which augmented AAA expansion and significantly increased aortic rupture rate). Zhang et al. (2018) identified miR-155 was upregulated in Ang II-infused ApoE-/- mice. Downregulation of miR-155 by antagomir could prevent the development of AAA by inhibiting macrophage inflammasome activation and cytokine expression. Also, Kim et al. (2014) observed that miR-712 was one of the most robustly upregulated miRNAs in Ang II-induced AAA mice model. Subsequent *in vivo* experiments showed that silencing of miR-712 significantly prevented the development of AAA by decreasing the aortic matrix metalloproteinases (MMPs) activity and inflammation. The study of Nakao et al. (2017) reported that deletion of miR-33a-5p attenuated AAA formation in both mouse models of Ang II- and calcium chloride-induced AAA, the mechanism of which was also associated with the reduction of p38 mitogen-activated protein kinase (MAPK)-mediated macrophage accumulation and MMP9 expression. However, the AAA-related miRNAs remain rarely reported.

In the present study, we aimed to further screen crucial miRNAs by integrating analysis of two miRNA microarray datasets that were performed in two mouse models. In addition, the predicted target genes of identified miRNAs were also confirmed to be differentially expressed in another one mRNA microarray dataset. Therefore, our identified miRNA-mRNA interaction pairs may be underlying important targets for treatment of AAA, which had not been performed previously.

Materials and Methods

Collection of microarray datasets

The expression profiles of AAA were retrieved from the public Gene Expression Omnibus (GEO) database (http://www.ncbi.nlm.nih.gov/geo/) under accession number GSE109639 (Furusho et al. 2018), GSE51229 (Maegdefessel et al. 2015) and GSE54943 (Kim et al. 2014), respectively. A total of 12 aortic samples in GSE109639 microarray dataset [Platform: GPL10787, Agilent-028005 SurePrint G3 Mouse GE 8x60K Microarray (Probe Name version)] were collected to analyze the mRNA expression profile, including 6 samples from wild type AAA mice that were induced by periaortic application of 0.5 M $CaCl_2$ for 7 days and 42 days and 6 from wild type mice undergoing sham operation in which mice were treated with physiological saline instead of $CaCl_2$ for 7 days and 42 days. A total of 10 aortic samples in GSE51229 microarray dataset [GPL10384, Agilent-021828 Unrestricted Mouse miRNA Microarray (V2)] were collected to investigate the miRNA expression profile, consisting of 5 from AAA mice that were induced by type I PPE (1.5 U/ml) for 7 days and 5 from sham operation that underwent saline infusion for 7 days. A total of 9 aortic samples in GSE54943 microarray dataset (GPL17075, miRCURY LNA microRNA Array, 6th generation – miRBase 16.0) were collected to explore the miRNA expression profile, containing 6 from 12 h and 36 h post-Ang II pump implanted mice and 3 from controls at 0 h Ang II pump implantation.

Data preprocessing and expression analysis

The raw expression data in TXT format were downloaded and preprocessed using the Linear Models for Microarray data (LIMMA) method (Ritchie et al. 2015) (version 3.34.0; http://www.bioconductor.org/packages/release/bioc/html/limma.html) in the Bioconductor R package (version 3.4.1; http://www.R-project.org/), including log transformation of data with a skewed distribution to approximate normal distribution and normalization by the quantile adjustment method.

The differentially expressed genes (DEGs) and miRNAs (DEMs) between AAA and controls were identified using the LIMMA method (Ritchie et al. 2015) (see Supplementary Information S1) based on the threshold value of $|\log_2 FC(\text{fold change})| > 1$ and false discovery rate (FDR) < 0.05. Bidirectional hierarchical clustering was conducted using the pheatmap in R package (version: 1.0.8; https://cran.r-project.org/web/packages/pheatmap) on the basis of Euclidean distance algorithm, the results of which was visualized as a heat map.

Protein-protein interaction (PPI) network construction and module analysis

The Search Tool for the Retrieval of Interacting Genes (STRING; version 10.0; http://string-db.org/) database (Szklarczyk et al. 2015) was used to predict the interaction relationships between DEGs. Only the interactors with confidence score ≥ 0.8 were considered to be significant and integrated to construct the PPI network using the Cytoscape software (version 3.6.1; www.cytoscape.org/) (Kohl et al. 2011). The CytoNCA plugin in cytoscape software (http://apps.cytoscape.org/apps/cytonca) (Tang et al. 2015) was utilized to calculate the topological features of the proteins in the PPI network, including degree centrality (DC), betweenness centrality (BC), closeness centrality (CC) and average path length (APL). The hub genes were selected if they were in the top 30 genes according to the above 4 ranking methods. Moreover, the Molecular Complex Detection (MCODE; version:1.4.2, http://apps.cytoscape.org/apps/mcode) (Bader and Hogue 2003) plugin of the Cytoscape software was used to screen modules from the PPI network with MCODE score > 3 and a node number > 5 set as the statistical criteria.

DEMs-DEGs interaction prediction

The target genes of DEMs were predicted using the miRWalk database (version 2.0; http: //www.zmf.umm.uni-heidelberg.

de/apps/zmf/mirwalk2) (Dweep and Gretz 2015) which provides the biggest collection of predicted and experimentally verified miR-target interactions with 12 miRNA databases (miRWalk, MicroT4, miRanda, miRBridge, miRDB, miRMap, miRNAMap, PICTAR2, PITA, RNA22, RNAhybrid, Targetscan). The target genes were then overlapped with the DEGs to screen the negative interaction relationships between DEMs and DEGs (that is, opposite expression), which was used for constructing the miRNA regulatory network.

Function enrichment analysis

In order to analyze the potential function of DEGs and DEMs, gene ontology (GO) enrichment for the biological process (BP), cellular component (CC), and molecular function (MF) categories and Kyoto Encyclopedia of Genes and Genomes (KEGG) pathway analysis were performed using the Database for Annotation, Visualization and Integrated Discovery (DAVID) (version 6.8; http://david.abcc.ncifcrf.gov) (Huang et al. 2009). A value $p < 0.05$ was considered statistically significant.

Results

Identification of DEGs and DEMs

Using FDR < 0.05 and $|\log_2 FC| > 1$ as the cut-off criteria, a total of 1407 DEGs were identified from GSE109639, including 672 upregulated and 735 downregulated genes between AAA and control mice (Fig. 1A; Table S1 in Sup-

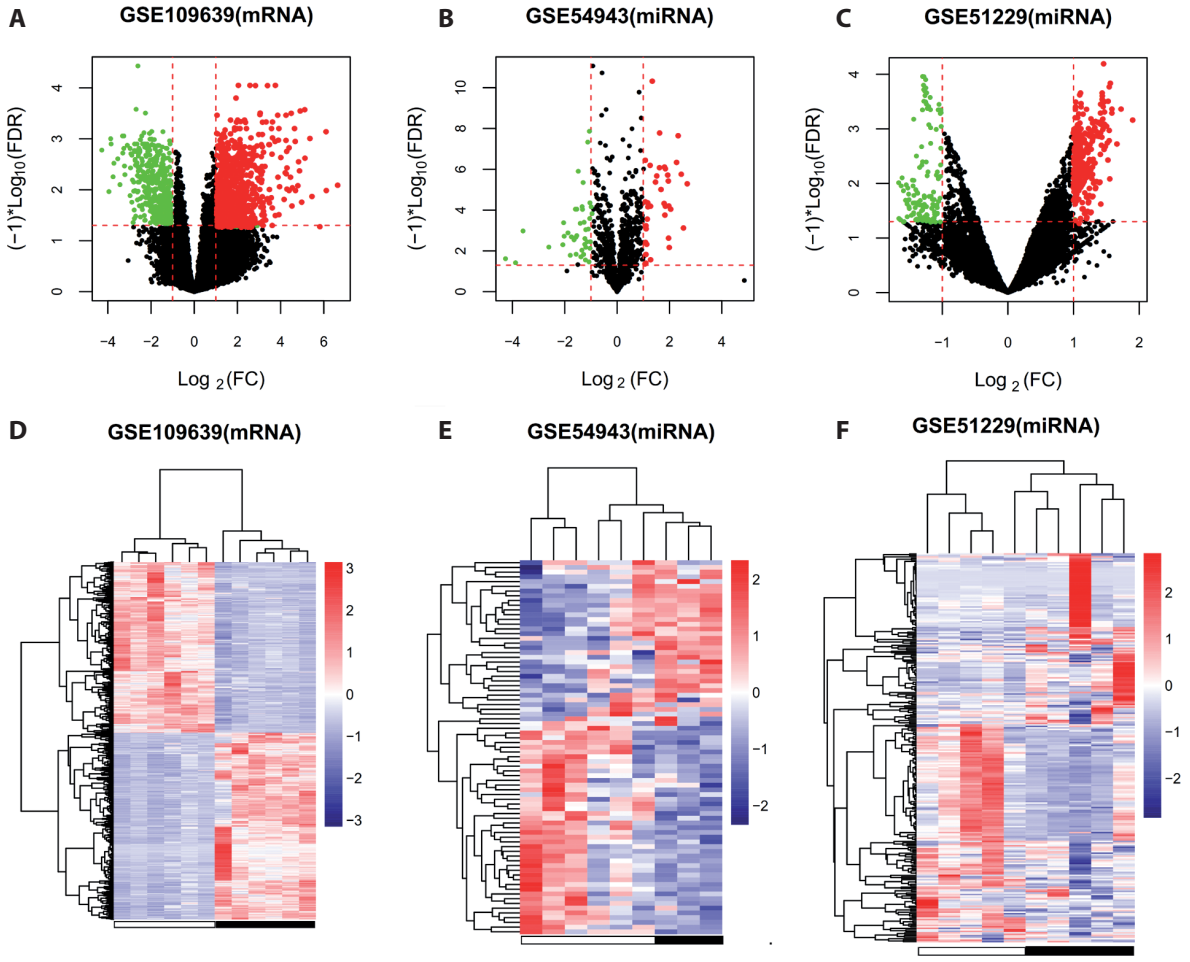

Figure 1. Volcano plot and heat map of differentially expressed genes and miRNAs. Volcano plot of differentially expressed genes in GSE109639 (**A**), miRNAs in GSE54943 (**B**) and GSE51229 (**C**) datasets. Red point indicated upregulated, while green point indicated downregulated differentially expressed RNAs. Black plots indicated no significant difference. Heat map of differentially expressed genes in GSE109639 (**D**), miRNAs in GSE54943 (**E**) and GSE51229 (**F**) datasets. Red cells represented high expression, while blue represented low expression. White box indicated the abdominal aortic aneurysm samples and black box indicated control samples. FDR, false discovery rate.

plementary Material); a total of 264 DEMs were identified from GSE51229, consisting of 141 upregulated and 123 downregulated miRNAs between AAA and control mice (Fig. 1B; Table S1); a total of 83 DEMs were identified from GSE54943, containing 53 upregulated and 30 downregulated miRNAs between AAA and control samples (Fig. 1C; Table S1). The heat map showed the mRNA (Fig. 1D) and miRNA (Fig. 1E,F) profiles had been significantly changed after AAA induction. Furthermore, the DEMs in two datasets were compared and 35 DEMs were found to be shared, with 18 having the consistent expression trend (Table 1).

Screening of crucial DEGs by PPI network and module analyses

Using the STRING online database and the threshold value of confidence score ≥ 0.8, a total of 490 DEGs (246 upregulated and 244 downregulated genes) were filtered to construct the PPI network, including 1477 edges (such as

Table 1. Common differentially expressed miRNAs in two datasets and hub/top genes

miRNAs	GSE51229		GSE54943		mRNAs	GSE109639	
	logFC	FDR	logFC	FDR		logFC	FDR
mmu-miR-30a	−1.66	4.23E-02	1.04	3.71E-02	*NTF3*	−1.89	2.65E-02
mmu-miR-376c	−4.08	4.64E-02	1.03	4.60E-02	*GNG2*	1.54	1.40E-02
mmu-miR-302b	2.50	4.46E-02	−1.04	4.22E-02	*ITGA7*	−2.02	3.28E-03
mmu-miR-193b	−2.24	4.26E-02	1.05	3.71E-02	*HEBP1*	−1.25	2.70E-02
mmu-miR-93	−8.24	5.89E-03	1.01	3.40E-02	*CCR2*	1.97	2.44E-02
mmu-miR-335-5p	2.90	4.79E-02	1.03	4.35E-02	*CCL5*	2.19	2.80E-02
mmu-miR-28	−5.65	8.33E-03	1.07	6.80E-03	*CXCL5*	4.89	1.80E-02
mmu-miR-17	2.66	2.30E-02	1.13	1.07E-02	*Igj*	6.78	7.93E-03
mmu-miR-302a	−4.15	1.47E-02	−1.07	6.20E-03	*S100a9*	6.3	9.64E-03
mmu-miR-705	1.74	2.69E-02	1.12	3.83E-03	*Igh-VJ558*	5.77	1.20E-02
mmu-miR-718	5.45	1.05E-02	−1.03	1.07E-02	*Stfa3*	5.62	1.43E-03
mmu-miR-92b	3.86	2.58E-02	1.06	4.43E-02	*Spp1*	5.36	4.73E-02
mmu-miR-763	−5.90	2.39E-02	1.11	2.50E-02	*Col11a1*	4.94	1.85E-03
mmu-miR-467a	2.64	1.70E-02	−1.03	2.98E-02	*Mmp13*	4.73	3.79 E-03
mmu-miR-18b	3.09	2.30E-03	−1.05	4.28E-02	*Il1b*	4.72	6.38 E-04
mmu-miR-133a	−1.76	4.55E-02	1.19	3.16E-02	*Cxcl3*	4.53	6.68 E-04
mmu-miR-20a	2.89	2.63E-02	1.14	1.36E-02	*Tnn*	4.5	6.04 E-03
mmu-miR-296-5p	2.24	1.54E-02	−1.09	2.46E-02	*Thbs4*	4.46	4.33 E-03
mmu-miR-155	6.06	5.34E-04	1.04	3.29E-02	*Anxa8*	4.43	1.04 E-02
mmu-miR-292-3p	−4.52	2.00E-02	−1.05	2.47E-02	*Cxcl14*	4.33	2.21 E-02
mmu-miR-411	2.37	4.52E-02	1.06	1.13E-03	*S100a8*	4.33	1.25 E-02
mmu-miR-714	−14.00	4.26E-04	1.07	2.95E-02	*Kng1*	4.32	2.05 E-03
mmu-miR-409-3p	3.45	2.83E-02	−1.06	4.66E-04	*Pkp1*	4.29	1.27E-03
mmu-miR-350	2.78	3.73E-02	1.06	8.25E-03	*Clec4e*	4.2	1.13E-02
mmu-miR-677	3.42	1.89E-02	1.06	2.74E-03	*Glycam1*	4.15	7.27E-04
mmu-miR-802	−3.36	3.31E-02	−1.01	1.03E-02	*AA467197*	4.12	7.67E-03
mmu-miR-294	−7.97	2.00E-03	−1.05	1.91E-02	*Il6*	4.06	1.25E-02
mmu-miR-431	6.75	1.79E-03	1.02	3.68E-02	*Cfi*	4.06	2.59E-03
mmu-miR-21	6.67	9.08E-04	1.17	4.18E-03	*Arg1*	3.97	1.19E-02
mmu-miR-201	−1.89	3.53E-02	1.04	3.30E-02	*Gjb3*	3.97	5.45E-03
mmu-miR-322	2.44	2.73E-02	1.02	2.17E-02	*Kng2*	3.96	2.97E-03
mmu-miR-205	−4.52	2.66E-02	−1.05	2.31E-02	*Slurp1*	3.94	6.74 E-03
mmu-miR-1197	4.92	4.60E-02	1.02	3.86E-02	*Gm5483*	3.93	7.82 E-04
mmu-miR-215	−2.19	3.45E-02	1.06	3.04E-02	*Prg4*	3.93	1.98 E-03
mmu-miR-208b	−4.12	2.47E-02	−1.03	3.87E-02	*Col2a1*	3.9	6.47 E-03

FC, fold change; FDR, false discovery rate.

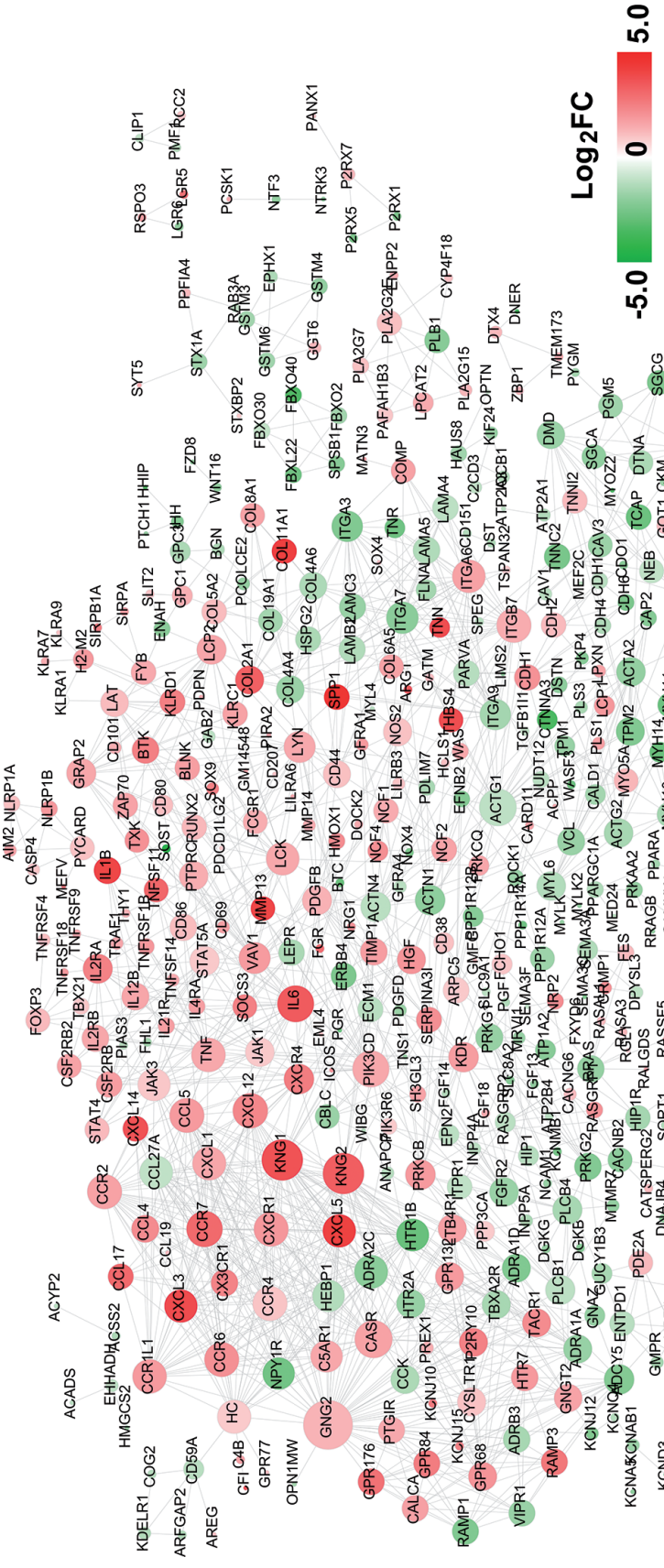

Figure 2. The protein and protein interaction network. Red, upregulated; green, downregulated. The larger size of node (protein) indicated the higher degree (interaction relationships) of it.

Table 2. Hub genes ranked by four topological features

Gene	DC	Gene	CC	Gene	BC	Gene	APL
GNG2	55	*PLB1*	1	*NTF3*	1	*NTF3*	1
KNG2	39	*PLA2G2E*	1	*SNRPN*	1	*SNRPN*	1
KNG1	39	*FBXO40*	1	*KERA*	1	*KERA*	1
CASR	32	*FBXL22*	1	*STX1A*	0.833	*STX1A*	1
ACTG1	31	*SPSB1*	1	*EHHADH*	0.833	*DTX4*	1
PIK3CD	30	*GSTM4*	1	*DTX4*	0.667	*P2RX7*	1
IL6	30	*STX1A*	1	*P2RX7*	0.667	*HAUS8*	1
CCR7	29	*GSTM6*	1	*HAUS8*	0.500	*PLB1*	1
CXCL12	27	*HAUS8*	1	*ACSS2*	0.500	*PLA2G2E*	1
CCR4	26	*FBXO2*	1	*PLB1*	0.246	*GSTM4*	1
ITGB7	26	*GSTM3*	1	*PLA2G2E*	0.246	*GSTM6*	1
CCR2	26	*FBXO30*	1	*ACTG1*	0.148	*GSTM3*	1
CCL5	26	*DTX4*	1	*PRKCB*	0.140	*FBXO40*	1
CXCR1	26	*P2RX7*	1	*GNG2*	0.136	*FBXL22*	1
CCR6	26	*LGR6*	1	*ITGB7*	0.104	*SPSB1*	1
TNF	25	*NTF3*	1	*PIK3CD*	0.102	*FBXO2*	1
CCR1L1	25	*SNRPN*	1	*NOS2*	0.082	*FBXO30*	1
ADRA2C	24	*PMF1*	1	*IL6*	0.076	*LGR6*	1
HC	24	*CLIP1*	1	*TNF*	0.072	*PMF1*	1
CXCL1	24	*RCC2*	1	*CDH1*	0.062	*CLIP1*	1
CCL27A	23	*RSPO3*	1	*LYN*	0.060	*RCC2*	1
LCK	23	*KERA*	1	*RRAS*	0.060	*RSPO3*	1
ITGA6	23	*LGR5*	1	*PDGFB*	0.057	*LGR5*	1
CXCL3	23	*PTPRZ1*	1	*GSTM4*	0.056	*PTPRZ1*	1
CXCL5	23	*RGS7BP*	1	*GSTM6*	0.056	*RGS7BP*	1
HTR1B	22	*BMX*	1	*GSTM3*	0.056	*BMX*	1
JAK3	22	*KCTD10*	1	*HGF*	0.055	*KCTD10*	1
NPY1R	21	*RPL18A*	1	*KDR*	0.054	*RPL18A*	1
ITGA7	21	*RGS7*	1	*LCK*	0.051	*RGS7*	1
HEBP1	21	*ACSL1*	1	*MYL6*	0.049	*ACSL1*	1

Top 35 genes ranked according to each topological feature were screened. DC, degree centrality; CC, closeness centrality; BC, betweenness centrality; APL, average path length.

GNG2 [guanine nucleotide binding protein (G protein), gamma 2]-*CCR2*[C-C motif chemokine receptor 2]/*CCL5* [C-C motif chemokine ligand 5]) (Fig. 2; Table S2). Among these 490 DEGs, *NTF3* [neurotrophin-3] was considered to be a hub gene because it was overlapped in the top 35 genes according to the 3 ranking methods (BC, CC, APL); *GNG2* may act as a hub gene because it was overlapped in DC and BC ranking; *ITGA7* [integrin subunit alpha 7], *CCL5* and *CCR2* were also believed to be crucial according to the DC ranking (Table 2).

The 490 DEGs were subjected to the DAVID database to predict their functions. As a result, 37 GO terms (21, BP; 12, CC; 4, MF) were enriched, such as GO:0006954~inflammatory response (*CXCL5*, *CCL5*, *HC*, *CCR2*), GO:0006928~cell motion (*NTF3*), GO:0007155~cell adhesion (ITGA7), GO:0022610~biological adhesion (*ITGA7*), GO:0008283~cell proliferation (*GNG2*) and GO:0042592~homeostatic process (*NTF3*) (Fig. 3; Table 3). Furthermore, 13 KEGG pathways were also enriched, such as mmu04510: Focal adhesion (*ITGA7*), mmu04062: Chemokine signaling pathway (*CXCL5*, *CCL5*, *CCR2*, *GNG2*), mmu04512: extracellular matrix (ECM)-receptor interaction (*ITGA7*), mmu04810: Regulation of actin cytoskeleton (*ITGA7*) and mmu04010: MAPK signaling pathway (*NTF3*) (Fig. 3; Table 3).

Moreover, 5 significant modules were extracted from the whole PPI network subsequently to further screen important genes for AAA. The results showed that hub gene *GNG2* with its interactors *CCL5* and *CCR2* were enriched in module 1, while hub gene *ITGA7* was enriched in mod-

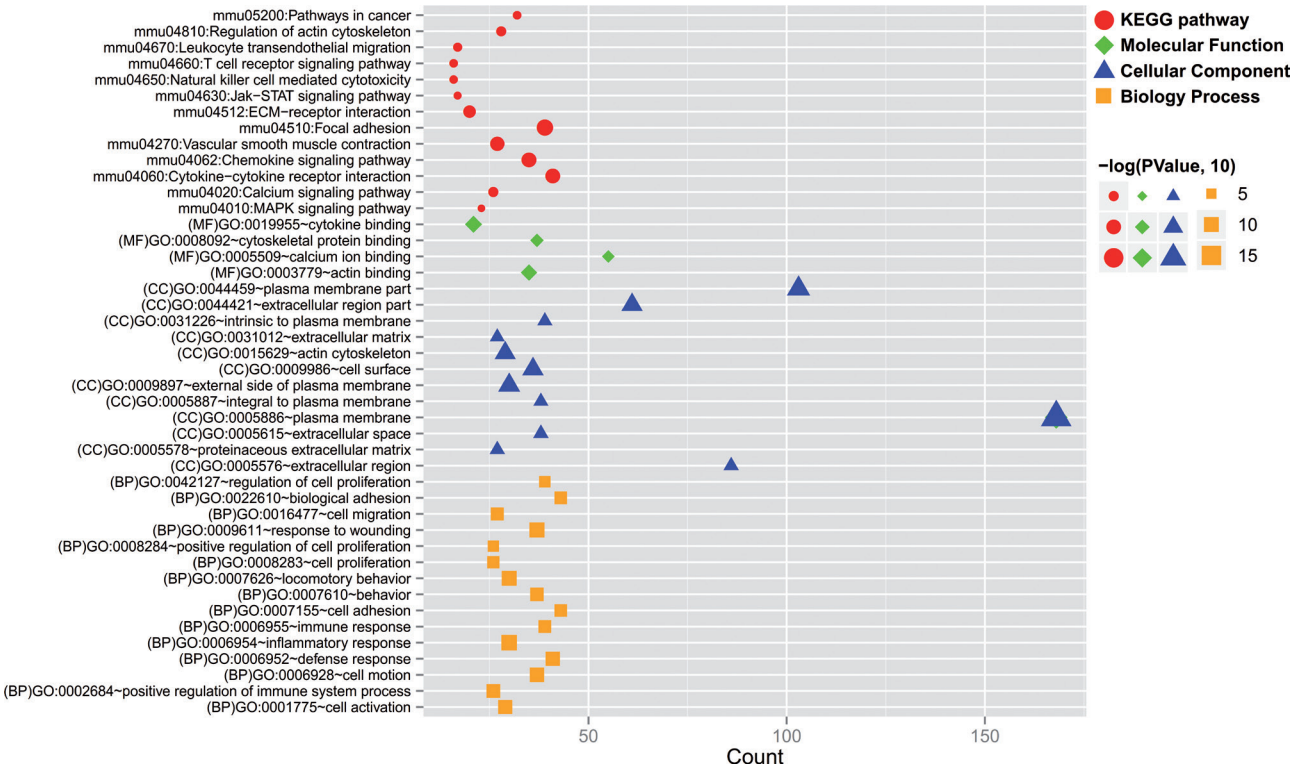

Figure 3. Function enrichment analysis for the genes in the protein and protein interaction network. KEGG, Kyoto encyclopedia of genes and genomes; GO, gene ontology; CC, cellular component; BP, biological process; MF, molecular function.

ule 3; the others were not enriched in significant modules (Fig. 4; Table 4).

Screening of crucial DEMs by miRNA-mRNA regulatory network analysis

A total of 130 DEGs (44 upregulated; 86 downregulated) were predicted to be negatively regulated by 6 DEMs (4 upregulated; 2 downregulated), which constituted the 139 interaction relationships (such as mmu-miR-677-*ITGA7*, mmu-miR-350-*NTF3* and mmu-miR-292-3p-*GNG2*) to construct the miRNA-mRNA regulatory network (Fig. 5). The target genes of these miRNAs were enriched into 24 GO terms (9, BP; 9, CC; 6, MF), such as GO:0048878~chemical homeostasis (*NTF3*), GO:0019838~growth factor binding (*NTF3*) and GO:0005509~calcium ion binding (*ITGA7*) (Fig. 6; Table 5). Furthermore, 4 KEGG pathways were also enriched, including mmu04512: ECM-receptor interaction (*ITGA7*) and mmu04510: Focal adhesion (*ITGA7*) (Fig. 6; Table 5).

Discussion

Although the pathogenesis of AAA is complex, recent studies suggest that progressive inflammation, vascular smooth muscle cell apoptosis and vessel wall destabilization play important roles in the development and progression of AAA (Kuivaniemi et al. 2015; Investigators 2017; Zhang et al. 2019). Thus, miRNAs that regulate these processes may be particularly crucial for AAA. As expected, in present study, we identified three important miRNAs (mmu-miR-292-3p, mmu-miR-350 and mmu-miR-677) in AAA. mmu-miR-292-3p regulated *GNG2* to participate in cell proliferation and Chemokine signaling pathway; mmu-miR-350 modulated *NTF3* to be involved in cell motion and MAPK signaling pathway; mmu-miR-677 could target *ITGA7* to affect ECM-receptor interaction.

GNG2 encodes a gamma subunit of the heterotrimeric G-protein complex GαGβγ. Previous studies demonstrated that inhibition of GαGβγ signaling retarded cancer cell growth, induced cell death (Bookout et al. 2003), alleviated the invasive phenotype (Ouelaa-Benslama 2012) and enhanced the chemosensitivity (Paudyal et al. 2017). Furthermore, using the zebrafish embryos as a model, Leung et al. (2006) also found that loss of *GNG2* inhibited angiogenesis by attenuating vascular endothelial growth factor (VEGF)-induced phosphorylation of phospholipase C-gamma1 and serine/threonine kinase signaling (Tinchung et al. 2006), while neutralization of VEGF was reported to suppress AAA formation (Glover 2013). These findings indicate that *GNG2* may be a proto-oncogene. This hypothesis can be indirectly

Table 3. Function enrichment for the genes in the PPI network

Category	Term	Count	*p*-value
BP			
	GO:0006954~inflammatory response	30	5.06E-11
	GO:0009611~response to wounding	37	1.28E-10
	GO:0007626~locomotory behavior	30	2.22E-10
	GO:0006928~cell motion	37	6.15E-10
	GO:0006952~defense response	41	1.09E-09
	GO:0001775~cell activation	29	1.99E-09
	GO:0002684~positive regulation of immune system process	26	3.98E-09
	GO:0007610~behavior	37	8.67E-09
	GO:0016477~cell migration	27	2.14E-08
	GO:0006955~immune response	39	4.57E-08
	GO:0007155~cell adhesion	43	7.15E-08
	GO:0022610~biological adhesion	43	7.51E-08
	GO:0008283~cell proliferation	26	1.52E-07
	GO:0007242~intracellular signaling cascade	58	1.89E-07
	GO:0007010~cytoskeleton organization	30	2.53E-07
	GO:0032989~cellular component morphogenesis	31	3.70E-07
	GO:0042592~homeostatic process	42	5.69E-07
	GO:0048870~cell motility	27	6.16E-07
	GO:0051674~localization of cell	27	6.16E-07
	GO:0042127~regulation of cell proliferation	39	1.32E-06
	GO:0008284~positive regulation of cell proliferation	26	2.08E-06
CC			
	GO:0005886~plasma membrane	168	3.66E-19
	GO:0044459~plasma membrane part	103	5.81E-13
	GO:0009897~external side of plasma membrane	30	6.44E-12
	GO:0009986~cell surface	36	1.63E-11
	GO:0044421~extracellular region part	61	2.31E-11
	GO:0015629~actin cytoskeleton	29	3.15E-11
	GO:0005615~extracellular space	38	1.16E-06
	GO:0005576~extracellular region	86	1.64E-06
	GO:0005578~proteinaceous extracellular matrix	27	1.64E-06
	GO:0031226~intrinsic to plasma membrane	39	2.81E-06
	GO:0005887~integral to plasma membrane	38	2.89E-06
	GO:0031012~extracellular matrix	27	3.42E-06
MF			
	GO:0019955~cytokine binding	21	8.28E-13
	GO:0003779~actin binding	35	5.39E-12
	GO:0008092~cytoskeletal protein binding	37	6.99E-09
	GO:0005509~calcium ion binding	55	5.36E-08
KEGG			
	mmu04510:Focal adhesion	39	5.36E-12
	mmu04062:Chemokine signaling pathway	35	1.67E-10
	mmu04060:Cytokine-cytokine receptor interaction	41	2.41E-10
	mmu04270:Vascular smooth muscle contraction	27	9.73E-10
	mmu04512:ECM-receptor interaction	20	7.47E-08
	mmu04020:Calcium signaling pathway	26	4.22E-05
	mmu04810:Regulation of actin cytoskeleton	28	5.15E-05
	mmu04670:Leukocyte transendothelial migration	17	7.66E-04
	mmu05200:Pathways in cancer	32	1.62E-03
	mmu04660:T cell receptor signaling pathway	16	1.98E-03
	mmu04650:Natural killer cell mediated cytotoxicity	16	2.76E-03
	mmu04630:Jak-STAT signaling pathway	17	9.32E-03
	mmu04010:MAPK signaling pathway	23	3.49E-02

GO, Gene ontology analysis; BP, biological process; CC, cellular component; MF, molecular function; KEGG, Kyoto Encyclopedia of Genes and Genomes.

Table 4. Module analysis

Cluster	Score	Node	Edges	Node IDs
1	10.455	22	230	*HEBP1, CCR6, HTR1B, CASR, CCL5, CXCR1, KNG1, CXCL3, CCR7, CXCL5, GNG2, ADRA2C, CCL27A, CXCL1, C5AR1, KNG2, CCR1L1, CCR4, CCR2, HC, CXCL12, NPY1R*
2	5	11	55	*CYSLTR1, ADRA1A, TACR1, LTB4R1, TBXA2R, GPR68, ADRA1D, CCK, P2RY10, GPR132, HTR2A*
3	4.188	16	67	*ITGA3, COL5A2, COL2A1, COL4A4, LAMC3, COL19A1, COL11A1, COL8A1, ITGA7, ITGA9, LAMB2, LAMA4, ITGB7, COL4A6, LAMA5, ITGA6*
4	3.739	23	86	*CSF2RB, CD80, LAT, IL2RB, JAK3, LYN, LCK, IL2RA, VAV1, LEPR, CXCR4, CD86, JAK1, TXK, STAT5A, IL6, SOCS3, BLNK, LCP2, ZAP70*
5	3	7	21	*SERPINA3I, ACTN1, PDGFB, ACTN4, ECM1, TIMP1, HGF*

Score = density × the number of nodes.

Figure 4. Significant modules extracted from the protein and protein interaction network. The larger size of node (protein) indicated the higher degree (interaction relationships) of it. M, module; red, upregulated; green, downregulated.

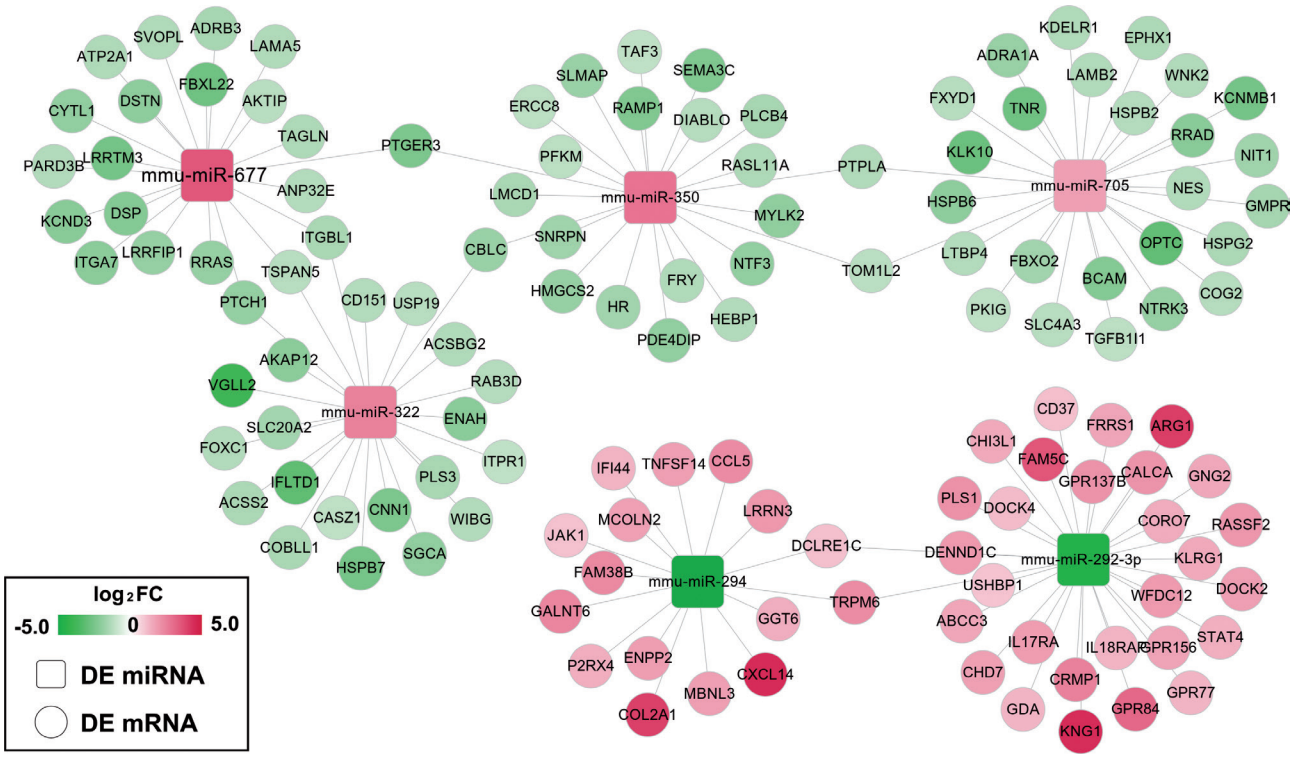

Figure 5. miRNA-mRNA interaction network. Square nodes represented miRNAs; circular nodes represented mRNAs. Red, upregulated; green, downregulated.

confirmed in a recent study of saliva exosomes in pancreatic cancer-bearing mice (Lau et al. 2013) and directly seen in the analysis results of neuroblastoma cells (Liu and Li 2019) and human AAA tissues (Gan et al. 2019) (all indicated *GNG2* was upregulated in cancer groups compared with controls). In line with these descriptions, our results showed that *GNG2* was upregulated in AAA model mice. However, the roles and mechanisms of *GNG2* in cancer remain rarely reported and even controversial (Naito 2012; Yajima et al. 2012, 2014). In our study, we predicted that *GNG2* may be involved in AAA development by inducing the inflammatory pathway because it was observed to interact with a serial of pro-inflammatory chemokines (*CCL5* and *CCR2*). This prediction result was also proved in the study of colorectal cancer (Liang et al. 2016) and human AAA (Gan et al. 2019). There was also evidence to display *CCL5* could accelerate tumor growth, migration and invasion (Wang et al. 2015) by promoting VEGF production and VEGF-dependent angiogenesis (Liu et al. 2014; Wang et al. 2016). *CCR2* mRNA and protein was similarly reported to be highly expressed in aggressive prostate cancer cells/tissues compared with less aggressive cancer or non-neoplastic cells/tissues. A high level of *CCR2* was correlated with higher clinical pathologic stage (Lu et al. 2007). RNA interference or antibody mediated inhibition of *CCR2* expression significantly inhibited tumorigenesis and blocked *CCR2*-induced migration and survival (Fang et al. 2012; Teng et al. 2017). Delayed angiogenesis and VEGF production was also observed in *CCR2*-deficiency mice (Ochoa et al. 2007). Accordingly, we believe *GNG2* may be involved in AAA *via CCL5*/*CCR2*-VEGF related inflammation-angiogenesis pathway. miRNAs (such as miR-292-3p) that regulated *GNG2* may be downregulated in AAA. The studies on miR-292-3p are relatively rare and there was no study to confirm the association between miR-292-3p and cancer development. However, miR-292-3p belongs to a member of miR-290. The previous study had shown that upregulation of miR-290 in two independent breast cancer cell lines significantly suppressed both primary tumor and metastatic growth (Goldberger et al. 2013), which indirectly demonstrated the tumor suppressor roles of miR-292-3p. Furthermore, research showed miR-292-5p was down-regulated in lung fibroblasts induced by TGF-β1 (Gao et al. 2020), while Cyclophilin A that induced the formation of AAA and thoracic aortic aneurysm by increased levels of TGF-β1 (Perrucci et al. 2020). This may also indirectly infer the downregulated expression of miR-292 in AAA.

NTF3 encodes a neurotrophic factor and thus, it was previously suggested to be elevated, like other growth factors (such as brain-derived neurotrophic factor), in cancer cells and tissues to promote colony growth, motility, migration

Table 5. Function enrichment analysis for the target genes of miRNAs

Category	Term	*p*-value	Genes
BP			
	GO:0008015~blood circulation	2.06E-04	*KNG1*, *CALCA*, *ADRB3*, *P2RX4*, *CHD7*, *ADRA1A*, *FOXC1*
	GO:0003013~circulatory system process	2.06E-04	*KNG1, CALCA, ADRB3, P2RX4, CHD7, ADRA1A, FOXC1*
	GO:0007507~heart development	7.30E-03	*CHD7, HSPG2, ADRA1A, SEMA3C, FOXC1, COL2A1, PTCH1*
	GO:0009628~response to abiotic stimulus	1.26E-02	*CALCA, DCLRE1C, ADRB3, ERCC8, HSPB6, HSPB7, HSPB2*
	GO:0042592~homeostatic process	1.39E-02	*CALCA, DCLRE1C, ADRB3, P2RX4, PTGER3, NTF3, ADRA1A, COL2A1, PTCH1, PFKM, ITPR1*
	GO:0048598~embryonic morphogenesis	2.02E-02	*ENAH, CHD7, LAMA5, HSPG2, FOXC1, COL2A1, PTCH1, TGFB1I1*
	GO:0048878~chemical homeostasis	2.19E-02	*CALCA, P2RX4, PTGER3, NTF3, ADRA1A, PTCH1, PFKM, ITPR1*
	GO:0044093~positive regulation of molecular function	3.00E-02	*CALCA, ADRB3, PTGER3, AKTIP, CYTL1, ADRA1A, DIABLO*
	GO:0006811~ion transport	4.58E-02	*FXYD1, P2RX4, KCND3, TRPM6, PTGER3, SLC20A2, ATP2A1, MCOLN2, SLC4A3, ITPR1, KCNMB1*
CC			
	GO:0044421~extracellular region part	3.32E-03	*KNG1, OPTC, LTBP4, CHI3L1, HSPG2, TNFSF14, COL2A1, CCL5, CALCA, ARG1, LAMB2, CXCL14, LAMA5, TNR, SEMA3C*
	GO:0005887~integral to plasma membrane	9.88E-03	*NTRK3, P2RX4, KCND3, ENPP2, ITGA7, ABCC3, BCAM, PTCH1, KCNMB1, SGCA, ITGBL1*
	GO:0031226~intrinsic to plasma membrane	1.27E-02	*NTRK3, P2RX4, KCND3, ENPP2, ITGA7, ABCC3, BCAM, PTCH1, KCNMB1, SGCA, ITGBL1*
	GO:0005578~proteinaceous extracellular matrix	3.18E-02	*OPTC, LAMB2, LAMA5, LTBP4, TNR, HSPG2, COL2A1*
	GO:0044459~plasma membrane part	3.28E-02	*GPR156, KCND3, TRPM6, ENAH, RAB3D, ENPP2, BCAM, KCNMB1, ITGBL1, NTRK3, P2RX4, ITGA7, ABCC3, DSP, RRAS, GNG2, PTCH1, PARD3B, TGFB1I1, SGCA, COG2*
	GO:0031012~extracellular matrix	3.74E-02	*OPTC, LAMB2, LAMA5, LTBP4, TNR, HSPG2, COL2A1*
	GO:0005576~extracellular region	4.24E-02	*KNG1, OPTC, NTF3, ENPP2, LTBP4, HSPG2, CHI3L1, TNFSF14, COL2A1, CCL5, ITGBL1, CALCA, ARG1, WFDC12, LAMB2, CXCL14, LAMA5, TNR, FAM5C, SEMA3C, PTCH1*
	GO:0005886~plasma membrane	4.54E-02	*GPR84, ENAH, RAB3D, SLC20A2, ENPP2, TNFSF14, RRAD, BCAM, KCNMB1, ITGBL1, ADRB3, SLMAP, RRAS, GNG2, PARD3B, GPR156, KCND3, TRPM6, PTGER3, NTF3, GPR77, NTRK3, P2RX4, AKTIP, ITGA7, ABCC3, ADRA1A, DSP, PTCH1, TGFB1I1, SGCA, COG2*
	GO:0000267~cell fraction	4.88E-02	*ADRB3, PLCB4, PKIG, ACSBG2, HSPB2, ADRA1A, EPHX1, CORO7, PFKM, ITPR1*
MF			
	GO:0019838~growth factor binding	1.67E-03	*NTRK3, IL18RAP, NTF3, LTBP4, COL2A1*
	GO:0005509~calcium ion binding	3.46E-02	*CBLC, STAT4, TRPM6, PLCB4, GALNT6, LTBP4, ATP2A1, ITGA7, PLS1, ITPR1, PLS3, SGCA*
	GO:0005216~ion channel activity	3.72E-02	*FXYD1, P2RX4, KCND3, TRPM6, MCOLN2, ITPR1, KCNMB1*
	GO:0022838~substrate specific channel activity	4.23E-02	*FXYD1, P2RX4, KCND3, TRPM6, MCOLN2, ITPR1, KCNMB1*
	GO:0022803~passive transmembrane transporter activity	4.47E-02	*FXYD1*, *P2RX4*, *KCND3*, *TRPM6*, *MCOLN2, ITPR1, KCNMB1*
	GO:0015267~channel activity	4.47E-02	*FXYD1*, *P2RX4*, *KCND3*, *TRPM6*, *MCOLN2*, *ITPR1*, *KCNMB1*
KEGG			
	mmu04020:Calcium signaling pathway	1.06E-03	*ADRB3*, *P2RX4*, *PLCB4*, *PTGER3*, *ATP2A1*, *ADRA1A*, *MYLK2*, *ITPR1*
	mmu04270:Vascular smooth muscle contraction	3.37E-03	*PLCB4*, *ADRA1A*, *MYLK2, RAMP1*, *ITPR1*, *KCNMB1*
	mmu04512:ECM-receptor interaction	5.26E-03	*LAMB2*, *LAMA5*, *TNR*, *ITGA7*, *COL2A1*
	mmu04510:Focal adhesion	2.59E-02	*LAMB2*, *LAMA5*, *TNR*, *ITGA7*, *MYLK2*, *COL2A1*

GO, Gene ontology analysis; BP, biological process; CC, cellular component; MF, molecular function; KEGG, Kyoto Encyclopedia of Genes and Genomes.

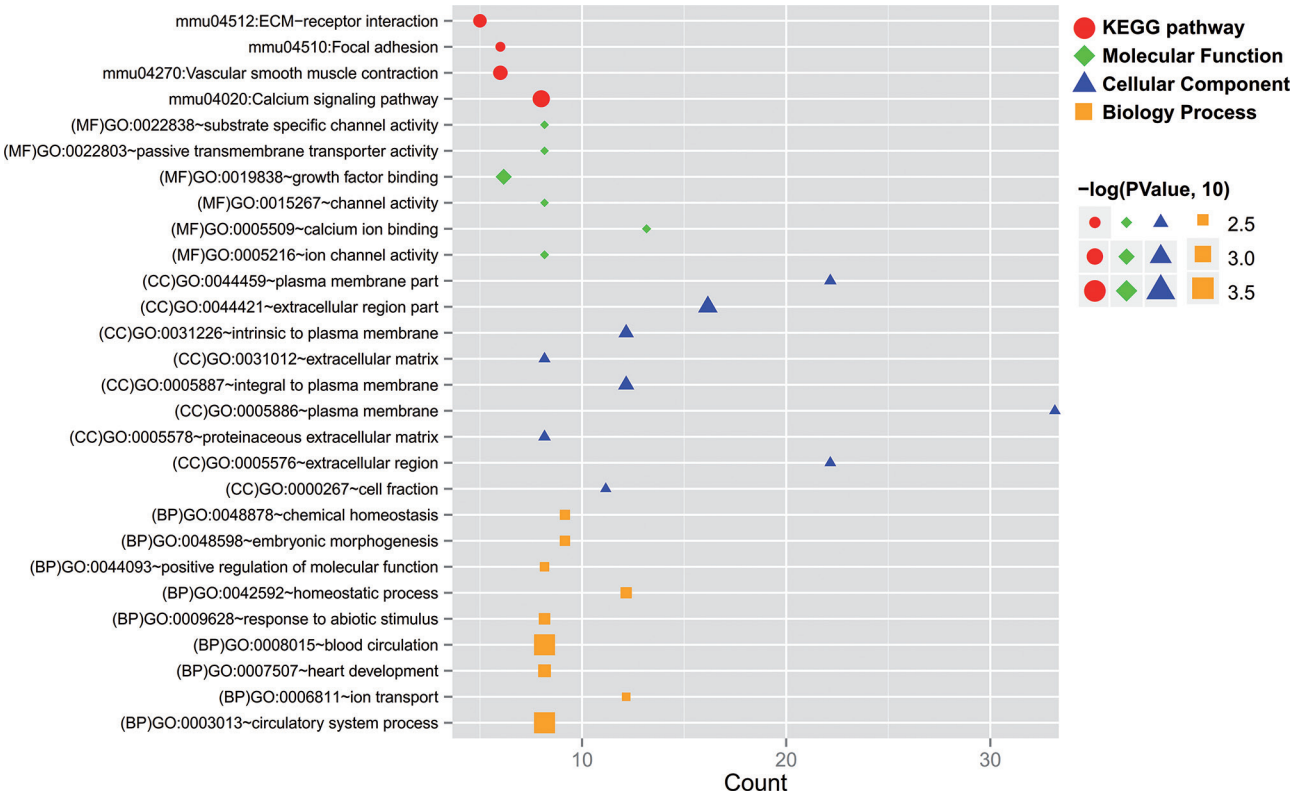

Figure 6. Function enrichment analysis for the genes in the miRNA-mRNA interaction network. KEGG, Kyoto encyclopedia of genes and genomes; GO, gene ontology; CC, cellular component; BP, biological process; MF, molecular function.

and invasion (Artico et al. 2012; Ivanov et al. 2013; Lawn et al. 2015; Liu et al. 2018). Targeted inhibition of *NTF3* may be an anti-tumoral strategy by triggering apoptosis of cancer cells (Bouzas-Rodriguez et al. 2010). However, recent studies indicate that NTF3may have a dual function of regulating the growth of cancer cells (Louie et al. 2013). The study of Kim et al. reported that *NTF3* induced a concentration-dependent increase in apoptosis in the medulloblastoma cell line (Kim et al. 1996). Ashour et al. (2013) also observed that overexpression of *NTF3* resulted in greater loss of the viability of medulloblastoma cells. In line with these two studies, we also found that *NTF3* was significantly downregulated in AAA model mice. According to the literature record, we also speculated the tumor suppressor roles of *NTF3* in AAA may be associated with its anti-inflammatory and immunomodulatory effects (Yalvac et al. 2016). Therefore, the function mechanisms of miR-350 that negatively regulated *NTF3* expression in AAA may correlate with the inflammatory and apoptosis process. This hypothesis was indirectly confirmed by the following studies: by bioinformatics analysis, upregulated miR-350 was found to regulate multiple inflammatory and apoptosis signaling pathways (including MAPK signaling pathway, NF-kappa B signaling pathway and apoptosis) to response to the toxicity of nano-TiO_2 exposure (Sui et al. 2018). Further gain- and loss-of-function analyses demonstrated that overexpression of miR-350 induced hypertrophy of cardiomyocytes through the posttranslational suppression of p38 and JNK protein synthesis and nuclear translocation of pro-inflammatory nuclear factor of activated T cells C3 (NFATC3) (Ge et al. 2013). Jiang et al. (2016) identified the expression of miR-350 was increased in mice bearing Lewis lung carcinoma compared with tumor-free control by microarray and RT-qPCR. The target genes regulated by miR-350 were enriched in the pathways of regulation of apoptotic process cell cycle and adaptive immune response.

ITGA7 encodes a member of the extracellular matrix proteins which are crucial compositions of vessel wall (Hungerford et al. 1996). Hereby, downregulation of *ITGA7* may lead to the destabilization and the dilation of vessel wall, ultimately resulting in the development of AAA and rupture. This tumor-suppressor potential of *ITGA7* was proved in our AAA samples and other cancers. For example, *ITGA7* was downregulated in breast cancer tissues compared to the adjacent normal tissues. *In vitro* experiments showed that knockdown of *ITGA7* significantly enhanced the migration and invasion of breast cancer cell lines by promoting the

expressions of c-met and vimentin (Bhandari et al. 2018). Laszlo et al. (2015) and Burkin and Fontelonga (2015) identified a significant reduction in *ITGA7* expression in malignant pleural mesothelioma cells. Forced expression of integrin α7 reversed the migratory phenotype of these cells. Multivariate analysis screened *ITGA7* expression as an independent prognostic factor, showing patients with high *ITGA7* expression having a longer median overall survival compared to the low- or no-expression groups. The report of Tan et al. (1996) revealed that *ITGA7* exerted tumor-suppressor roles in prostate cancer cells by binding to tissue inhibitor of metalloproteinase 3 (TIMP3) and then decreasing tumor necrosis factor α, cytoplasmic translocation of NF-κB, and of cyclin D1. However, the roles and regulatory mechanisms (such as miRNAs) of *ITGA7* remain rarely reported. In this study, we identified mmu-miR-677 may be an important upstream regulator for *ITGA7*. The studies on miR-677 in cancer are also not investigated previously, indicating it may represent a novel target for AAA.

There were some limitations in this study. First, the AAA model was induced by different methods in our included datasets. This may result in the association between miRNAs and mRNAs that could not be directly evaluated and only estimated according to their expression trend. Also, most of the miRNAs were only expressed in specific models, not overlapped in two datasets. Thus, the mRNA and miRNA profiles using the same model background should be further explored to confirm the relationship between our identified miRNAs and mRNAs. Second, we only preliminarily predicted the targeted relationships between miRNAs and mRNAs and their involved biological processes in AAA. Further wet experiments need to be performed to validate their interactions (luciferase reporter assay, knockout or overexpression *in vitro* or *in vivo* and PCR) and their influence on the development of AAA (analysis of inflammatory cells and cytokines, cell apoptosis, proliferation and AAA rupture rates) (Suehiro et al. 2019; Fashandi et al. 2020).

In conclusion, our present study suggests mmu-miR-677-*ITGA7*, mmu-miR-350-*NTF3* and mmu-miR-292-3p-*GNG2* interaction pairs may represent novel mechanisms for explaining the pathogenesis of AAA. Targeted regulation of them may be potential strategies for treatment of AAA.

Availability of data and materials. The microarray data GSE109639, GSE51229 and GSE54943 were downloaded from the GEO database in NCBI (http://www.ncbi.nlm.nih.gov/geo/).

Funding. This study was supported by Special Disease of Vasculitis in Pudong New Area (PWZzb2017-07); The Outstanding Clinical Discipline Project of Shanghai Pudong (PWYgy-2018-08); Program for Medical Key Department of Shanghai (ZK2019A10).

Conflict of interests. The authors declare that they have no competing interests.

References

Artico M, Bianchi E, Magliulo G, De Vincentiis M, De Santis E, Orlandi A, Santoro A, Pastore FS, Giangaspero F, Caruso R, et al. (2012): Neurotrophins, their receptors and KI-67 in human GH-secreting pituitary adenomas: an immunohistochemical analysis. Int. J. Immunopathol. Pharmacol. **25,** 117-125 https://doi.org/10.1177/039463201202500114

Ashour AE, Jamal S, Cheryan VT, Muthu M, Zoheir KM, Alafeefy AM, Abd-Allah AR, Levi E, Tarca AL, Polin LA, Rishi AK (2013): CARP-1 functional mimetics: a novel class of small molecule inhibitors of medulloblastoma cell growth. PloS One **8,** e66733 https://doi.org/10.1371/journal.pone.0066733

Bader GD, Hogue CW (2003): An automated method for finding molecular complexes in large protein interaction networks. BMC Bioinformatics **4,** 2 https://doi.org/10.1186/1471-2105-4-2

Bhandari A, Xia E, Zhou Y, Guan Y, Xiang J, Kong L, Wang Y, Yang F, Wang O, Zhang X (2018): ITGA7 functions as a tumor suppressor and regulates migration and invasion in breast cancer. Cancer Manag. Res. **10,** 969-976 https://doi.org/10.2147/CMAR.S160379

Bookout AL, Finney AR, Guo R, Peppel K, Koch WJ, Daaka Y (2003): Targeting Gbetagamma signaling to inhibit prostate tumor formation and growth. J. Biol. Chem. **278,** 37569-37573 https://doi.org/10.1074/jbc.M306276200

Bouzas-Rodriguez J, Cabrera JR, Delloye-Bourgeois C, Ichim G, Delcros JG, Raquin MA, Rousseau R, Combaret V, Bénard J, Tauszig-Delamasure S, Mehlen P (2010): Neurotrophin-3 production promotes human neuroblastoma cell survival by inhibiting TrkC-induced apoptosis. J. Clin. Invest. **120,** 850-858 https://doi.org/10.1172/JCI41013

Burkin DJ, Fontelonga TM (2015): Mesothelioma cells breaking bad: loss of integrin α7 promotes cell motility and poor clinical outcomes in patients. J. Pathol. **237,** 282-284 https://doi.org/10.1002/path.4587

Dereziński TL, Fórmankiewicz B, Migdalski A, Brazis P, Jakubowski G, Woda Ł, Jawień A (2017): The prevalence of abdominal aortic aneurysms in the rural/urban population in central Poland - Gniewkowo Aortic Study. Kardiol. Pol. **75,** 705-710 https://doi.org/10.5603/KP.a2017.0071

Dweep H, Gretz N (2015): miRWalk2.0: a comprehensive atlas of microRNA-target interactions. Nat. Methods **12,** 697 https://doi.org/10.1038/nmeth.3485

Fang WB, Jokar I, Zou A, Lambert D, Dendukuri P, Cheng N (2012): CCL2/CCR2 chemokine signaling coordinates survival and motility of breast cancer cells through Smad3 protein- and p42/44 mitogen-activated protein kinase (MAPK)-dependent mechanisms. J. Biol. Chem. **287,** 36593-36608 https://doi.org/10.1074/jbc.M112.365999

Fashandi AZ, Spinosa M, Salmon M, Su G, Montgomery W, Mast A, Lu G, Hawkins RB, Cullen JM, Sharma AK, et al. (2020): Female mice exhibit abdominal aortic aneurysm protection in an established rupture model. J. Surg. Res. **247,** 387-396 https://doi.org/10.1016/j.jss.2019.10.004

Furusho A, Aoki H, Ohno-Urabe S, Nishihara M, Hirakata S, Nishida N, Ito S, Hayashi M, Imaizumi T, Hiromatsu S (2018):

Involvement of B cells, immunoglobulins, and syk in the pathogenesis of abdominal aortic aneurysm. J. Am. Heart Assoc. **7,** e007750
https://doi.org/10.1161/JAHA.117.007750

Gan S, Pan Y, Mao J (2019): miR-30a-GNG2 and miR-15b-ACSS2 interaction pairs may be potentially crucial for development of abdominal aortic aneurysm by influencing inflammation. DNA Cell. Biol. **38,** 1540-1556
https://doi.org/10.1089/dna.2019.4994

Gao X, Xu D, Li S, Wei Z, Li S, Cai W, Mao N, Jin F, Li Y, Yi X, et al. (2020): Pulmonary silicosis alters microRNA expression in rat lung and miR-411-3p exerts anti-fibrotic effects by inhibiting MRTF-A/SRF signaling. Mol. Ther. Nucleic Acids **20,** 851-865
https://doi.org/10.1016/j.omtn.2020.05.005

Ge Y, Pan S, Guan D, Yin H, Fan Y, Liu J, Zhang S, Zhang H, Feng L, Wang Y, et al. (2013): MicroRNA-350 induces pathological heart hypertrophy by repressing both p38 and JNK pathways. Biochim. Biophys. Acta **1832,** 1-10
https://doi.org/10.1016/j.bbadis.2012.09.004

Glover KJ, Xu B, Iida Y, Xuan H, Tanaka H, Wang W, Naoki Fujimura N, Gerritsen M, Dalman RL (2013): VEGF-A neutralization suppresses experimental abdominal aortic aneurysm (AAA) formation. J. Vasc. Surg. **57,** 84S
https://doi.org/10.1016/j.jvs.2013.02.200

Goldberger N, Walker RC, Kim CH, Winter S, Hunter KW (2013): Inherited variation in miR-290 expression suppresses breast cancer progression by targeting the metastasis susceptibility gene Arid4b. Cancer Res. **73,** 2671-2681
https://doi.org/10.1158/0008-5472.CAN-12-3513

Huang DW, Sherman BT, Lempicki RA (2009): Systematic and integrative analysis of large gene lists using DAVID bioinformatics resources. Nat. Protoc. **4,** 44-57
https://doi.org/10.1038/nprot.2008.211

Hungerford JE, Owens GK, Argraves WS, Little CD (1996): Development of the aortic vessel wall as defined by vascular smooth muscle and extracellular matrix markers. Dev. Biol. **178,** 375-392
https://doi.org/10.1006/dbio.1996.0225

Investigators MRS (2017): Aortic wall inflammation predicts abdominal aortic aneurysm expansion, rupture, and need for surgical repair. Circulation **136,** 787-797
https://doi.org/10.1161/CIRCULATIONAHA.117.028433

Ivanov SV, Panaccione A, Brown B, Guo Y, Moskaluk CA, Wick MJ, Brown JL, Ivanova AV, Issaeva N, El-Naggar AK, Yarbrough WG (2013): TrkC signaling is activated in adenoid cystic carcinoma and requires NT-3 to stimulate invasive behavior. Oncogene **32,** 3698-3710
https://doi.org/10.1038/onc.2012.377

Jiang J, Gao Q, Wang T, Lin H, Zhan Q, Chu Z, Huang R, Zhou X, Liang X, Guo W (2016): MicroRNA expression profiles of granulocytic myeloid-derived suppressor cells from mice bearing Lewis lung carcinoma. Mol. Med. Rep. **14,** 4567-4574
https://doi.org/10.3892/mmr.2016.5845

Johansson G, Swedenborg J (2010): Ruptured abdominal aortic aneurysms: a study of incidence and mortality. Br. J. Surg. **73,** 101-103
https://doi.org/10.1002/bjs.1800730205

Kent KC (2014): Clinical practice: Abdominal aortic aneurysms. N. Engl. J. Med. **371,** 2101-2108
https://doi.org/10.1056/NEJMcp1401430

Kim CW, Kumar S, Son DJ, Jang IH, Griendling KK, Jo H (2014): Prevention of abdominal aortic aneurysm by anti-microRNA-712 or anti-microRNA-205 in angiotensin II-infused mice. Arterioscler. Thromb. Vasc. Biol. **34,** 1412-1421
https://doi.org/10.1161/ATVBAHA.113.303134

Kim YH, Cho SH, Lee SJ, Choi SA, Phi JH, Kim SK, Wang KC, Cho BK, Kim CY (1996): Growth-inhibitory effect of neurotrophin-3-secreting adipose tissue-derived mesenchymal stem cells on the D283-MED human medulloblastoma cell line. J. Neurooncol. **106,** 89-98
https://doi.org/10.1007/s11060-011-0656-8

Kohl M, Wiese S, Warscheid B (2011): Cytoscape: software for visualization and analysis of biological networks. Methods Mol. Biol. **696,** 291-303
https://doi.org/10.1007/978-1-60761-987-1_18

Kuivaniemi H, Ryer EJ, Elmore JR, Tromp G (2015): Understanding the pathogenesis of abdominal aortic aneurysms. Expert. Rev. Cardiovasc. Ther. **13,** 975-987
https://doi.org/10.1586/14779072.2015.1074861

Laszlo V, Hoda MA, Garay T, Pirker C, Ghanim B, Klikovits T, Dong YW, Rozsas A, Kenessey I, Szirtes I, et al. (2015): Epigenetic down-regulation of integrin α7 increases migratory potential and confers poor prognosis in malignant pleural mesothelioma. J. Pathol. **2,** 203-214
https://doi.org/10.1002/path.4567

Lau C, Kim Y, Chia D, Spielmann N, Eibl G, Elashoff D, Wei F, Lin YL, Moro A, Grogan T, et al. (2013): Role of pancreatic cancer-derived exosomes in salivary biomarker development. J. Biol. Chem. **288,** 26888-26897
https://doi.org/10.1074/jbc.M113.452458

Lawn S, Krishna N, Pisklakova A, Qu X, Fenstermacher DA, Fournier M, Vrionis FD, Tran N, Chan JA, Kenchappa RS, Forsyth PA (2015): Neurotrophin signaling via TrkB and TrkC receptors promotes the growth of brain tumor-initiating cells. J. Biol. Chem. **290,** 3814-3824
https://doi.org/10.1074/jbc.M114.599373

Leung T, Chen H, Stauffer AM, Giger KE, Sinha S, Horstick EJ, Humbert JE, Hansen CA, Robishaw JD (2006): Zebrafish G protein gamma2 is required for VEGF signaling during angiogenesis. Blood **108,** 160-166
https://doi.org/10.1182/blood-2005-09-3706

Liang B, Li C, Zhao J (2016): Identification of key pathways and genes in colorectal cancer using bioinformatics analysis. Med. Oncol. **33,** 111
https://doi.org/10.1007/s12032-016-0829-6

Lieberg J, Pruks LL, Kals M, Paapstel K, Aavik A, Kals J (2017): Mortality after elective and ruptured abdominal aortic aneurysm surgical repair: 12-year single-center experience of Estonia. Scand. J. Surg. **107,** 152-157
https://doi.org/10.1177/1457496917738923

Liu D, Song L, Dai Z, Guan H, Kang H, Zhang Y, Yan W, Zhao X, Zhang S (2018): MiR-429 suppresses neurotrophin-3 to alleviate perineural invasion of pancreatic cancer. Biochem. Biophys. Res. Commun. **505,** 1077-1083
https://doi.org/10.1016/j.bbrc.2018.09.147

Liu GT, Chen HT, Tsou HK, Tan TW, Fong YC, Chen PC, Yang WH, Wang SW, Chen JC, Tang CH (2014): CCL5 promotes VEGF-dependent angiogenesis by down-regulating miR-200b through PI3K/Akt signaling pathway in human chondrosarcoma cells. Oncotarget **5,** 10718-10731 https://doi.org/10.18632/oncotarget.2532

Liu J, Li Y (2019): Upregulation of MAPK10, TUBB2B and RASL11B may contribute to the development of neuroblastoma. Mol. Med. Rep. **20,** 3475-3486 https://doi.org/10.3892/mmr.2019.10589

Louie E, Chen XF, Coomes A, Ji K, Tsirka S, Chen EI (2013): Neurotrophin-3 modulates breast cancer cells and the microenvironment to promote the growth of breast cancer brain metastasis. Oncogene **32,** 4064-4077 https://doi.org/10.1038/onc.2012.417

Lu Y, Cai Z, Xiao G, Liu Y, Keller ET, Yao Z, Zhang J (2007): CCR2 expression correlates with prostate cancer progression. J. Cell Biochem. **101,** 676-685 https://doi.org/10.1002/jcb.21220

Maegdefessel L, Azuma J, Toh R, Merk DR, Deng A, Chin JT, Raaz U, Schoelmerich AM, Raiesdana A, Leeper NJ, et al. (2012): Inhibition of microRNA-29b reduces murine abdominal aortic aneurysm development. J. Clin. Invest. **122,** 497-506 https://doi.org/10.1172/JCI61598

Maegdefessel L, Spin JM, Raaz U, Eken SM, Toh R, Azuma J, Adam M, Nakagami F, Heymann HM, Chernogubova E (2015): Erratum: miR-24 limits aortic vascular inflammation and murine abdominal aneurysm development. Nat. Commun. **5,** 5214 https://doi.org/10.1038/ncomms6214

Naito Y (2012): Reduced GNG2 expression levels in mouse malignant melanomas and human melanoma cell lines. Am. J. Cancer Res. **2,** 322-329

Nakao T, Horie T, Baba O, Nishiga M, Nishino T, Izuhara M, Kuwabara Y, Nishi H, Usami S, Nakazeki F (2017): Genetic ablation of microRNA-33 attenuates inflammation and abdominal aortic aneurysm formation via several anti-inflammatory pathways. Arterioscler. Thromb. Vasc. Biol. **4,** 2161-2170 https://doi.org/10.1161/ATVBAHA.117.309768

Ochoa O, Sun D, Reyes-Reyna SM, Waite LL, Michalek JE, Mcmanus LM, Shireman PK (2007): Delayed angiogenesis and VEGF production in CCR2-/- mice during impaired skeletal muscle regeneration. Am. J. Physiol. Regul. Integr. Comp. Physiol. **293,** R651-661 https://doi.org/10.1152/ajpregu.00069.2007

Ouelaa-Benslama R, De Wever O, Hendrix A, Sabbah M, Lambein K, Land D, Prévost G, Bracke M, Hung MC, Larsen AK, et al. (2012): Identification of a GαGβγ, AKT and PKCα signalome associated with invasive growth in two genetic models of human breast cancer cell epithelial-to-mesenchymal transition. Int. J. Oncol. **41,** 189-200

Paudyal P, Xie Q, Vaddi PK, Henry MD, Chen S (2017): Inhibiting G protein βγ signaling blocks prostate cancer progression and enhances the efficacy of paclitaxel. Oncotarget **8,** 36067-36081 https://doi.org/10.18632/oncotarget.16428

Perrucci GL, Rurali E, Corlianò M, Balzo M, Piccoli M, Moschetta D, Pini A, Gaetano R, Antona C, Egea G, et al. (2020): Cyclophilin A/EMMPRIN axis is involved in pro-fibrotic processes associated with thoracic aortic aneurysm of marfan syndrome patients. Cells **9,** 154 https://doi.org/10.3390/cells9010154

Ritchie ME, Phipson B, Wu D, Hu Y, Law CW, Shi W, Smyth GK (2015): limma powers differential expression analyses for RNA-sequencing and microarray studies. Nucleic Acids Res. **43,** e47 https://doi.org/10.1093/nar/gkv007

Sui J, Fu Y, Zhang Y, Ma S, Yin L, Pu Y, Liang G (2018): Molecular mechanism for miR-350 in regulating of titanium dioxide nanoparticles in macrophage RAW264.7 cells. Chem. Biol. Interact. **280,** 77-85 https://doi.org/10.1016/j.cbi.2017.12.020

Suehiro C, Suzuki J, Hamaguchi M, Takahashi K, Nagao T, Sakaue T, Uetani T, Aono J, Ikeda S, Okura T, et al. (2019): Deletion of interleukin-18 attenuates abdominal aortic aneurysm formation. Atherosclerosis **289,** 14-20 https://doi.org/10.1016/j.atherosclerosis.2019.08.003

Szklarczyk D, Franceschini A, Wyder S, Forslund K, Heller D, Huerta-Cepas J, Simonovic M, Roth A, Santos A, Tsafou KP (2015): STRING v10: protein-protein interaction networks, integrated over the tree of life. Nucleic Acids Res. **43,** D447-452 https://doi.org/10.1093/nar/gku1003

Tan LZ, Song Y, Nelson J, Yu YP, Luo JH (1996): Integrin α7 binds tissue inhibitor of metalloproteinase 3 to suppress growth of prostate cancer cells. Am. J. Pathol. **183,** 831-840 https://doi.org/10.1016/j.ajpath.2013.05.010

Tang Y, Li M, Wang J, Pan Y, Wu FX (2015): CytoNCA: a cytoscape plugin for centrality analysis and evaluation of protein interaction networks. Biosystems **127,** 67-72 https://doi.org/10.1016/j.biosystems.2014.11.005

Teng KY, Han J, Zhang X, Hsu SH, He S, Wani NA, Barajas JM, Snyder LA, Frankel WL, Caligiuri MA, et al. (2017): Blocking the CCL2-CCR2 axis using CCL2-neutralizing antibody is an effective therapy for hepatocellular cancer in a mouse model. Mol. Cancer Ther. **16,** 312-322 https://doi.org/10.1158/1535-7163.MCT-16-0124

Tinchung L, Hui C, Stauffer AM, Giger KE, Soniya S, Horstick EJ, Humbert JE, Hansen CA, Robishaw JD (2006): Zebrafish G protein gamma2 is required for VEGF signaling during angiogenesis. Blood **108,** 160-166 https://doi.org/10.1182/blood-2005-09-3706

Wang LH, Lin CY, Liu SC, Liu GT, Chen YL, Chen JJ, Chan CH, Lin TY, Chen CK, Xu GH, et al. (2016): CCL5 promotes VEGF-C production and induces lymphangiogenesis by suppressing miR-507 in human chondrosarcoma cells. Oncotarget **7,** 36896-36908 https://doi.org/10.18632/oncotarget.9213

Wang SW, Liu SC, Sun HL, Huang TY, Chan CH, Yang CY, Yeh HI, Huang YL, Chou WY, Lin YM, Tang CH (2015): CCL5/CCR5 axis induces vascular endothelial growth factor-mediated tumor angiogenesis in human osteosarcoma microenvironment. Carcinogenesis **36,** 104-114 https://doi.org/10.1093/carcin/bgu218

Yajima I, Kumasaka MY, Yamanoshita O, Zou C, Li X, Ohgami N, Kato M (2014): GNG2 inhibits invasion of human malignant melanoma cells with decreased FAK activity. Am. J. Cancer Res. **4,** 182-188

Yajima I, Kumasaka MY, Naito Y, Yoshikawa T, Takahashi H, Funasaka Y, Suzuki T, Kato M (2012): Reduced GNG2 expression levels in mouse malignant melanomas and human melanoma cell lines. Am. J. Cancer Res. **2,** 322-329

Yalvac ME, Arnold WD, Braganza C, Chen L, Mendell JR, Sahenk Z (2016): AAV1.NT-3 gene therapy attenuates spontaneous autoimmune peripheral polyneuropathy. Gene Therapy **23,** 95-102 https://doi.org/10.1038/gt.2015.67

Zhang Z, Liang K, Zou G, Chen X, Shi S, Wang G, Zhang K, Li K, Zhai S (2018): Inhibition of miR-155 attenuates abdominal aortic aneurysm in mice by regulating macrophage-mediated inflammation. Biosci. Rep. **38,** BSR20171432 https://doi.org/10.1042/BSR20171432

Zhang Z, Zou G, Chen X, Lu W, Liu J, Zhai S, Qiao G (2019): Knockdown of lncRNA PVT1 inhibits vascular smooth muscle cell apoptosis and extracellular matrix disruption in a murine abdominal aortic aneurysm model. Mol. Cells **42,** 218-227

Received: June 7, 2020
Final version accepted: August 27, 2020

doi: 10.4149/gpb_2020033

Supplementary Material

miRNAs regulating the expressions of NTF3, GNG2 and ITGA7 are involved in the pathogenesis of abdominal aortic aneurysm in mice

Shujie Gan[1], Weijun Shi[2] and Jingdong Tang[2]

[1] *Department of Vascular Surgery, Shanghai General Hospital, Shanghai Jiao Tong University School of Medicine, Shanghai, China*
[2] *Department of Vascular Surgery, Shanghai Pudong Hospital, Fudan University Pudong Medical Center, Shanghai, China*

Supplementary Information S1. Rscript source code of Limma package

```
library(Biobase)
library(GEOquery)
library(limma)

# load series and platform data from GEO

gset <- getGEO("GSE57691", GSEMatrix =TRUE)
if (length(gset) > 1) idx <- grep("GPL96", attr(gset, "names")) else idx <- 1
gset <- gset[[idx]]

# make proper column names to match toptable
fvarLabels(gset) <- make.names(fvarLabels(gset))

# group names for all samples
sml                                                                                                    <-
c("G0","G1","G1","G1","G1","G0","G1","G0","G0","G0","G1","G0","G1","G0","G1","G1");

# log2 transform
ex <- exprs(gset)
qx <- as.numeric(quantile(ex, c(0., 0.25, 0.5, 0.75, 0.99, 1.0), na.rm=T))
LogC <- (qx[5] > 100) ||
              (qx[6]-qx[1] > 50 && qx[2] > 0) ||
              (qx[2] > 0 && qx[2] < 1 && qx[4] > 1 && qx[4] < 2)
if (LogC) { ex[which(ex <= 0)] <- NaN
  exprs(gset) <- log2(ex) }
```

```
# set up the data and proceed with analysis
fl <- as.factor(sml)
gset$description <- fl
design <- model.matrix(~ description + 0, gset)
colnames(design) <- levels(fl)
fit <- lmFit(gset, design)
cont.matrix <- makeContrasts(G1-G0, levels=design)
fit2 <- contrasts.fit(fit, cont.matrix)
fit2 <- eBayes(fit2, 0.01)
tT <- topTable(fit2, adjust="fdr", sort.by="B", number=250)

# load NCBI platform annotation
gpl <- annotation(gset)
platf <- getGEO(gpl, AnnotGPL=TRUE)
ncbifd <- data.frame(attr(dataTable(platf), "table"))
```

Table S1. Differentially expressed miRNAs and genes

GSE109639				GSE51229				GSE54943			
GENE_SYMBOL	logFC	FDR	P.Value	GENE_SYMBOL	logFC	FDR	P.Value	GENE_SYMBOL	logFC	FDR	P.Value
Sost	-4.28	0.001673	4.19E-06	mmu-miR-714	-14.0047	0.000426	6.207E-05	mmu-miR-409-3p	-1.06177285	0.000466	5.81E-05
Mylk4	-3.95	0.010895	1.91E-04	mmu-miR-183	-10.6045	0.001775	0.0002586	mmu-miR-3082-3p	-1.03832161	0.000593	7.40E-05
Slc22a2	-3.87	0.000999	9.34E-07	mmu-miR-883a-3p	-10.0766	0.002283	0.0003326	mmu-miR-3062	1.1008746	0.00081	0.000101
Slc22a1	-3.85	0.001272	2.15E-06	mmu-miR-669i	-9.86712	0.002529	0.0003685	mmu-miR-411	1.05600325	0.001135	0.000141
Vgll2	-3.76	0.005554	5.95E-05	mmu-miR-217	-9.74059	0.002692	0.0003922	mmu-miR-24	-1.0279223	0.00205	0.000256
Tmem200b	-3.72	0.003013	1.70E-05	mmu-miR-465c-5p	-9.42547	0.003153	0.0004594	mmu-miR-1193-5p	-1.03933815	0.002497	0.000311
Dner	-3.54	0.002483	1.13E-05	mmu-miR-323-5p	-9.08288	0.00376	0.0005478	mmu-miR-677	1.06137859	0.00274	0.000342
Ctnna3	-3.44	0.007933	1.12E-04	mmu-miR-466g	-8.80243	0.004356	0.0006347	mmu-miR-705	1.11935001	0.00383	0.000478
Myoz2	-3.32	0.000882	6.32E-07	mmu-miR-296-3p	-8.34574	0.005572	0.0008118	mmu-miR-1-1	1.0380437	0.003939	0.000491
Fbxo40	-3.31	0.001906	5.83E-06	mmu-miR-93	-8.24435	0.005891	0.0008583	mmu-miR-21	1.16588396	0.004182	0.000522
E030013I19Rik	-3.26	0.001554	3.51E-06	mmu-miR-294	-7.9693	0.002001	0.0002915	mmu-miR-374	-1.07051492	0.00429	0.000535
Cidea	-3.26	0.000882	6.24E-07	mmu-miR-615-5p	-7.05325	0.004618	0.0006728	mmu-miR-879	1.01489099	0.005687	0.000709
Hhip	-3.23	0.003425	2.25E-05	mmu-miR-1899	-6.94712	0.005324	0.0007757	mmu-miR-302a	-1.07485882	0.006202	0.000773
Abra	-3.21	0.005056	4.94E-05	mmu-miR-220	-6.87808	0.003397	0.0004949	mmu-miR-9	-1.04297815	0.006371	0.000794
Slc9a2	-3.1	0.001341	2.43E-06	mmu-miR-717	-6.83368	0.013351	0.0019452	mmu-miR-28	1.07195558	0.006801	0.000848
Ptprz1	-3.05	0.001272	1.79E-06	mmu-miR-32	-6.80084	0.013621	0.0019846	mmu-miR-598	-1.02959478	0.006947	0.000866
Ifltd1	-3.01	0.002078	7.47E-06	mmu-miR-685	-6.74807	0.006217	0.0009058	mmu-miR-511-3p	1.03148641	0.007073	0.000882
Casq1	-2.97	0.013032	2.54E-04	mmu-miR-491	-6.2908	0.018693	0.0027236	mmu-miR-350	1.05967684	0.008251	0.001029
Optc	-2.97	0.001554	3.37E-06	mmu-miR-743b-5p	-6.07846	0.021392	0.0031168	mmu-miR-224	1.08333615	0.008721	0.001087
Gm16485	-2.95	0.003712	2.73E-05	mmu-miR-763	-5.90485	0.023918	0.0034849	mmu-miR-471-5p	1.16191678	0.009271	0.001156
Jph2	-2.93	0.001957	6.61E-06	mmu-miR-694	-5.90415	0.023928	0.0034863	mmu-miR-466h-3p	1.09552869	0.010197	0.001272

Table S2. Protein-protein interaction relationships

#Node1	Node2	Combined score	#Node1	Node2	Combined score	#Node1	Node2	Combined score
Cxcl12	Cxcr4	0.999	Htr2a	Tacr1	0.915	Casr	Cxcr1	0.9
Ncf1	Ncf2	0.999	Cxcr1	Cxcl3	0.915	Col2a1	Pcolce2	0.9
Lcp2	Vav1	0.999	Ldhb	Aldoc	0.915	Anapc7	Il6	0.9
Lcp2	Grap2	0.999	Cald1	Acta2	0.915	Gpr84	Gpr176	0.9
Stat5a	Jak1	0.998	Itga7	Comp	0.915	Plb1	Lpcat2	0.9
Tnfrsf1b	Tnf	0.998	Cysltr1	Htr2a	0.914	Kng2	Ccr6	0.9
S100a9	S100a8	0.998	Il4i1	Ddo	0.914	Ramp1	Gng2	0.9
Erbb4	Nrg1	0.998	Cxcl12	Hebp1	0.914	Cog2	Kdelr1	0.9
Stat5a	Jak3	0.998	Sgcd	Pgm5	0.914	Tacr1	Gpr132	0.9
Tnni2	Tnnc2	0.997	Cysltr1	Adra1a	0.914	Adrb3	Ramp3	0.9
Pik3cd	Rras	0.997	Dner	Dtx4	0.914	Actn4	Timp1	0.9
Lcp2	Fyb	0.997	Atp1a2	Fxyd7	0.914	Ccl27a	Kng1	0.9
Ntf3	Ntrk3	0.997	Jak3	Cxcr4	0.914	Gng2	Vipr1	0.9
Il2rb	Il2ra	0.997	Adcy5	Pde3a	0.914	Fcho1	Hip1	0.9
Lcp2	Lat	0.997	Myh10	Myh11	0.914	Ecm1	Serpina3i	0.9
Lck	Ptprc	0.996	Ccr7	Hc	0.914	Ramp1	Gpr176	0.9
Socs3	Il6	0.996	Adra1d	Adra1a	0.914	Htr1b	Cxcr1	0.9
Il1b	Il1r2	0.996	Myh14	Myh10	0.914	Plb1	Pafah1b3	0.9
Il1rl1	Il33	0.995	Pik3cd	Fgr	0.913	Adra2c	Cxcl1	0.9
Lcp2	Zap70	0.995	Plcb1	Dgkg	0.913	Fbxl22	Spsb1	0.9
Lck	Vav1	0.995	Fbxl22	Fbxo2	0.913	Ccr4	Npy1r	0.9
Pygm	Pgm5	0.994	Tnf	Tnfsf14	0.913	Gng2	Pik3r6	0.9
Lat	Vav1	0.993	Dgkg	Plcb4	0.913	Ecm1	Actn4	0.9
Blnk	Btk	0.993	Csf2rb2	Il2rb	0.913	Htr7	Gpr176	0.9
Il1b	Tnf	0.992	Blnk	Zap70	0.913	Cxcl3	Kng1	0.9
Klrd1	Klrc1	0.992	Htr7	Vipr1	0.913	Ccr6	Npy1r	0.9
Fyb	Grap2	0.991	C5ar1	Cxcl1	0.913	Fcho1	Arpc5	0.9
Lyn	Vav1	0.991	Thbs4	Pdgfb	0.913	Ccr4	C5ar1	0.9
Il1b	Il6	0.991	C5ar1	Cxcl5	0.913	Pla2g2e	Pafah1b3	0.9
Socs3	Lepr	0.99	Htr7	Adcy5	0.913	Hspa2	Sun1	0.9
Flna	Itgb7	0.99	Ccl27a	Cxcl5	0.913	Gpr68	Tacr1	0.9
Lat	Zap70	0.99	Adcy5	Gpr176	0.913	Haus8	Optn	0.9
Jak3	Il2ra	0.99	Klrd1	Btk	0.913	Hspa2	Sun2	0.9
Blnk	Vav1	0.99	Ramp1	Ramp3	0.912	Ccr1l1	Cxcl3	0.9
Jak1	Socs3	0.989	Tbxa2r	Cck	0.912	Kng2	Cxcl1	0.9
Tpm2	Acta2	0.989	Fyb	Enah	0.912	Adra2c	Cxcl5	0.9
Btk	Vav1	0.988	Sgca	Pgm5	0.912	Cacnb2	Catsperg2	0.9
Lcp2	Lck	0.988	Fgfr2	Hgf	0.912	Gng2	Cxcl1	0.9